

# Study on Aerodynamic Characteristics Between Right Turning Vehicles and Straight Running Vehicles

Hongtao Tang<sup>1</sup>, Daoxian Tong<sup>1</sup>, Xiang Zhang<sup>1</sup>, Honglin Chen<sup>1</sup> & Nenghui Zhou<sup>2</sup>

<sup>1</sup> College of Mechanical Engineering, Tianjin University of Science & Technology, Tianjin 300222, China

<sup>2</sup> Tianjin Yidingfeng Power Technology Co., Ltd., Tianjin 300380, China

Correspondence: Daoxian Tong, College of Mechanical Engineering, Tianjin University of Science & Technology, Tianjin 300222, China.

doi:10.56397/IST.2023.03.05

## Abstract

The dynamic meshing technology in computational fluid dynamics (CFD) is used to simulate the transient overtaking process of right turning vehicles and straight running vehicles. The characteristic of flow field around the vehicle model and the variation trend of lateral force and yawing moment are obtained. The research shows that when the speed of the straight vehicle increases, its lateral force and the yawing moment of both vehicles increase, while the lateral force of the right turning vehicle increases first and then decreases; The turning radius of the right turning vehicle increases, the lateral force of the two vehicles and the yawing moment of the straight vehicle decrease linearly, and the yawing moment of the right turning vehicle increases linearly.

**Keywords:** overtake, dynamic mesh, turn right, aerodynamics

## 1. Introduction

When two vehicles meet or overtake at a certain speed, the flow field around the body interferes with each other, resulting in continuous changes in the aerodynamic force of the vehicle, which not only seriously affects the aerodynamic balance of the car, but also affects the stability, safety and comfort of the vehicle when driving.

C. Noger obtained the change trend of aerodynamic forces during overtaking and the relative position of the vehicle when the flow field interaction is most obvious through a series of wind tunnel experiments. AZIM used smoke visualization methods to experiment with the overtaking process. The results show that the turbulence characteristics around the vehicle change significantly with the change of Reynolds number. HOWELL found in the overtaking test of cars and trucks that the pressure field at the head of the truck has an extremely critical effect on the load it is subjected to, while the pressure field at the head of the truck is only related to the speed of the truck. R.J. Corin used computational fluid dynamics to study the influence of vehicle relative velocity and crosswind on transient aerodynamics, and obtained the overall trend of aerodynamics during overtaking. In the study of the aerodynamic characteristics of the overtaking process, Fu Limin obtained the relative position of the vehicle when the overtaking resistance, lateral force and yaw moment reached the maximum. Wu Yunzhu found in the transient simulation of the overtaking process of the car that with the increase of relative speed, the lateral force coefficient and the yaw moment coefficient of the overtaken car increased linearly. Hu Xingjun found in the transient simulation of the influence of lateral spacing on the aerodynamic characteristics of overtaking: the smaller the lateral spacing between the two workshops, the stronger the aerodynamic interference. Tang Hongtao used dynamic grid technology to complete the transient simulation of various working conditions such as lane change overtaking and double-lane overtaking of cars, and obtained the influence of changes in relative vehicle speed and lateral spacing on the flow field under complex working conditions.

Past studies have focused on the mutual interference of the flow field of straight-going vehicles; However, there

are few published research literature on the flow field change and safety risk analysis of the common working condition of forced right turn. In this paper, the transient simulation of the overtaking process of right-turning vehicles and straight-going vehicles is carried out using dynamic grid technology, the pressure changes are analyzed, and the changes of lateral force and yaw moment are obtained, which provides theoretical guidance for people's safe driving and automatic driving technology.

**2. Basic Control Equations**

In the design scheme of this paper, the maximum car speed is 81km/h, and the Mach number is about 0.06617, which is less than 0.3, so it can be considered that the gas is incompressible.

Continuity equation:

$$\frac{\partial \rho}{\partial t} + \frac{\partial(\rho u)}{\partial x} + \frac{\partial(\rho v)}{\partial y} + \frac{\partial(\rho \omega)}{\partial z} = 0 \tag{1}$$

where  $\rho$  is the density; t is time;  $u, v,$  and  $\omega$  are velocity vectors in the X, Y, and Z directions, respectively.

Momentum conservation equation:

$$\frac{\partial}{\partial x_i} (u_i u_j) = - \frac{\partial p}{\partial x_j} + \frac{\partial}{\partial x_j} \left[ \mu_{ef} \left( \frac{\partial u_i}{\partial x_j} + \frac{\partial u_j}{\partial x_i} \right) \right] \tag{2}$$

where  $i, j = 1, 2, 3;$   $\mu_{ef}$  is the turbulent viscosity coefficient.

**3. Numerical Simulation**

*3.1 Selection of Car Models and Setting of Calculation Fields*

The car model uses a certain family SUV, its basic dimensions are length 4653mm, width 1886mm, height 1730mm. According to the size proportion of the car model, it is simplified to a flat rectangle, the length of the rectangle is represented by L, the width of the rectangle is represented by W, and the edges and corners of the front and rear of the car are arced according to the proportion. In order to ensure that the wall effect will not occur due to the narrow calculation domain during the simulation calculation process, and the overtaking process can be fully simulated, the size of the calculation domain is designed as 30L long and 50W wide. This is shown in Figure 1.

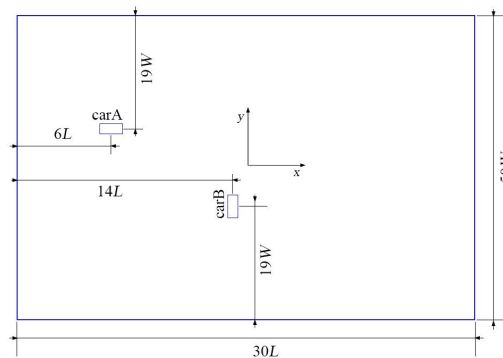


Figure 1. Vehicle model and computing domain

*3.2 Meshing*

The triangular unstructured mesh is used for simulation, the mesh size of the automobile body line is set to 0.1m, and the surface grid size of the calculation domain is set to 0.5m, and the total number of meshes is about 340000. As shown in Figure 2, the grid near the body is dense, which ensures the calculation accuracy of the computing domain around the body, so that the simulation is closer to the real motion state of the car. The edge area grid away from the body is sparse, in order to save computing resources and improve computing efficiency.

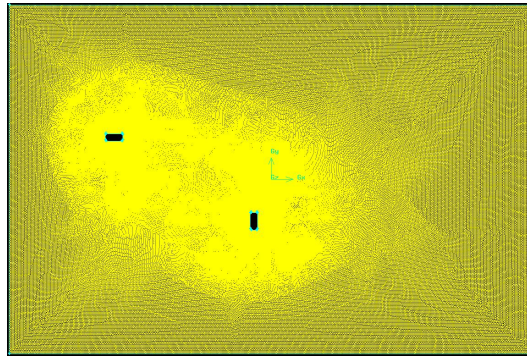


Figure 2. Mesh model

3.3 Setting of Boundary Conditions and Initial Conditions

The left boundary of the calculation domain is the pressure inlet, and the right boundary is the pressure outlet; Selection of transient solvers; The calculation model adopts the standard K-epsilon turbulence model; Fluid material selection ideal-gas. Simulate using Smoothing and Remeshing in moving meshes; The elasticity factor of the four parameters of Smoothing is set to 0.05, and the other three parameters remain at default values; In Remeshing, Must Improve Skewness and Size Function are used. The motion of the model is defined using UDFs; The type of model is Rigid Body, and the center of gravity position is the initial position of the model.

3.4 Overtaking Scheme Design

Remember that the distance between the center of car A and the center of car B in the positive direction of the x-axis is X, the distance along the positive direction of the y-axis is Y, and the angle of rotation of the car B body is, and the position of the two cars is indicated by X/L, Y/W. The car B model in case 2 was used to simulate the right turn process of one car, and it was compared with the overtaking process to verify the mutual influence of the two vehicles.

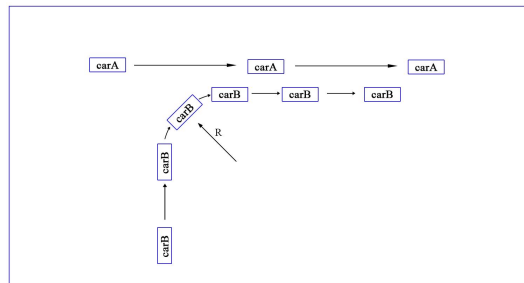


Figure 3. Schematic diagram of driving trajectory

Table 1. Design scheme

case	Speed of car A /(m • s <sup>-1</sup> )	Speed of car B /(m • s <sup>-1</sup> )	radius /(m)
case 1	/	=8	5
case 2	=12.5	=8	5
case 3	=15	=8	5
case 4	=17.5	=8	5
case 5	=20	=8	5
case 6	=22.5	=8	5
case 7	=15	=8	6
case 8	=15	=8	7
case 9	=15	=8	8
case 10	=15	=8	9

### 3.5 Analysis of Simulation Results

Taking case 1 and case 3 as examples, the lateral force and the yaw moment are compared and analyzed.

#### 3.5.1 Lateral Force Analysis

The lateral forces in this article are the forces perpendicular to the body of the surrounding airflow acting on the body. The positive direction of the lateral force is from the right side of the vehicle to the left and the negative direction is from the left side of the car body to the right.

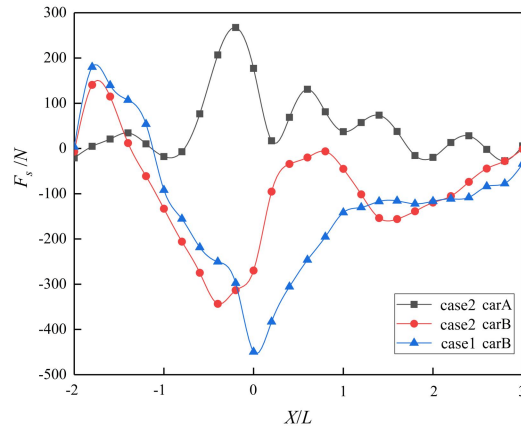


Figure 4. Lateral force

During the right turn of one car, there are two peaks in the lateral force of car B, the first of which occurs around  $X/L=-1.8$ ; The second occurs around  $X/L=0$ , and its value is about 2.5 times of the first peak, which has a certain adverse effect on driving; in the process of  $X/L=-2$  to  $X/L=1$ , the lateral force changes more sharply, affecting the driving stability and safety of car B; In the process of  $X/L=1$  to  $X/L=3$ , car B gradually gets rid of the flow field interference caused by the right turn, and its lateral force gradually approaches zero.

In the process of overtaking, disturbed by the car B flow field, the lateral force of car A increases rapidly from  $X/L=-0.8$ , reaching a maximum around  $X/L=-0.2$ , at which time car A has a tendency to slide to the left; As car A gradually surpasses car B in the x direction, its lateral force decreases rapidly. After  $X/L=2$ , the lateral force gradually stabilizes.

During the overtaking process, the lateral force change trend of car B is basically the same as that of one car turning right. However, due to the flow field interference of car A, the lateral force of car B changes significantly: the two peaks have decreased to varying degrees, especially the second peak, whose value is reduced by about 25%, and the adverse effects of the driving process are reduced; The first peak appears basically unchanged, and the second peak appears earlier, around  $X/L=-0.4$ . In the process of  $X/L=0.5$  to  $X/L=2.5$ , the lateral force changes greatly again, and car B has a tendency to shift to the right. After  $X/L=2.5$ , the lateral force of car B gradually approaches zero.

#### 3.5.2 Yaw Moment Analysis

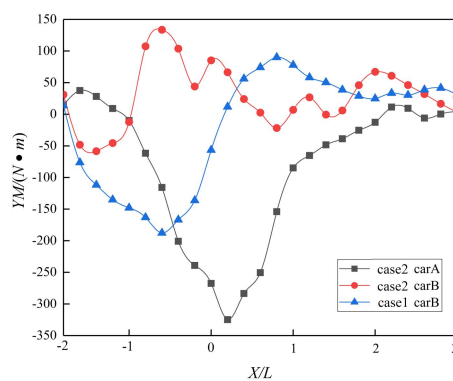


Figure 5. Yaw moment

In the process of turning right of the vehicle, the overall rotation direction of the body is clockwise, if the yaw moment is negative, that is, the direction is clockwise, the direction of body rotation is the same as the direction of the torque, to a certain extent, it is conducive to the body to complete the right turn action; If the yaw moment is positive, it is not conducive to the body completing the right turn action. The torque continues to increase before  $X/L=-0.3$ , the direction is negative, and the torque reaches a maximum value near  $X/L=-0.3$ , and then decreases rapidly; At  $X/L=0$ , the torque changes direction begins to increase, reaching an extreme value around  $X/L=0.6$ ; After that, the torque gradually decreases and approaches zero. When car B turns right, the direction of body rotation is basically the same as the direction of torque, which is conducive to completing the right turn action.

During overtaking, the torque of car B reaches a maximum value around  $X/L=-0.3$  and its direction is positive; In the process of  $X/L=0$  to  $X/L=1.5$ , the torque value is small; Subsequently, under the influence of the car A wake, the torque increases rapidly, reaching an extreme value around  $X/L=2$ , and then decreasing and approaching zero. During the overtaking process, affected by the flow field of car A, the torque direction of car B changes from clockwise to counterclockwise when cycling, which is not conducive to the completion of car B's right-turn action.

The yaw moment of car A continues to decrease before  $X/L=0.2$ , and the maximum value is obtained around  $X/L=0.2$ , and the direction is negative, and its value is about twice the maximum value of car B, which adversely affects the driving stability of car A. After that, the torque gradually decreases, approaching zero around  $X/L=3$ .

**4. The Effect of the Speed of a Straight-Going Vehicle on the Safety of the Vehicle**

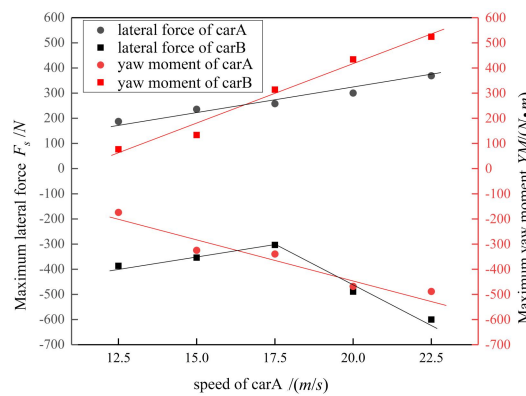


Figure 6. Maximum lateral force and yaw moment at different car A speeds

**4.1 Maximum Lateral Force Analysis**

With the increase of car A speed, the maximum lateral force of car A increases nearly linearly, and the lateral force of car B shows a trend of first decreasing and then increasing. Compared with 12.5m/s, when the speed of car A is 15m/s, 17.5m/s, 20m/s, and 22.5m/s, the maximum lateral force of car A increases in turn: 25.97%, 37.77%, 60.24%, and 97.02%. The maximum lateral force of car B changes as follows: when the speed of car A is 15m/s and 17.5m/s, the maximum lateral force decreases by 8.49% and 22.77% compared with the speed of 12.5m/s. When the speed of car A is 20m/s and 22.5m/s, and the maximum lateral force ratio is 17.5m/s, it increases by 61.22% and 83.97% respectively.

**4.2 Maximum Yaw Moment Analysis**

With the linear increase of car A speed, the maximum yaw moment of the two vehicles increases linearly. Compared with the speed of 12.5m/s, when the speed of car A is 15m/s, 17.5m/s, 20m/s, and 22.5m/s, the maximum yaw moment of car A increases by 86.45%, 94.98%, 168.64% and 180.33% respectively. The maximum yaw torque of car B increased by 73.36%, 307.65%, 463.62% and 580.61%.

In summary, during the overtaking process of right-turning vehicles and straight-going vehicles, the increase of car A speed has the greatest impact on the yaw torque of car B: the speed of car A is increased by 80%, and the maximum yaw torque of car B is increased by 580.61%, which adversely affects the stability and safety of car B.

**5. The Effect of Turning Radius on Vehicle Driving Safety**

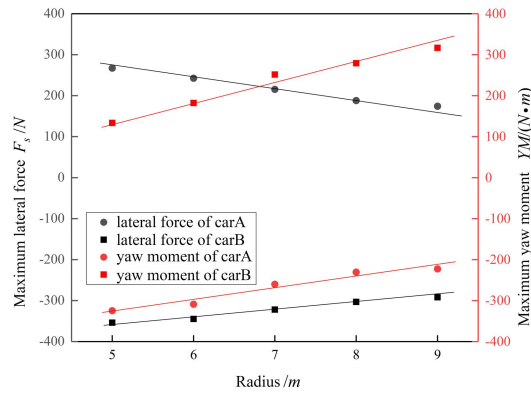


Figure 7. Maximum lateral force and yaw moment at different radii

### 5.1 Maximum Lateral Force Analysis

With the linear increase of the radius of the car B curve, the maximum lateral force of car A and car B decreases almost linearly. Compared with the turning radius of 5m, when the turning radius is 6m, 7m, 8m, and 9m, the maximum lateral force of car A decreases in turn: 9.24%, 19.37%, 29.62%, 34.18%; The maximum lateral force of car B decreased: 2.54%, 9.02%, 14.33%, 17.53%.

### 5.2 Maximum Yaw Moment Analysis

With the linear increase of the radius of the bend of car B, the maximum yaw moment of car A decreases nearly linearly, and the maximum yaw moment of car B increases nearly linearly. Compared with the turning radius of 5m, when the turning radius is 6m, 7m, 8m, 9m, the maximum yaw moment of car A decreases in turn: 4.91%, 19.85%, 28.99%, 31.41%; The maximum yaw moment of car B increased sequentially: 36.38%, 88.46%, 109.09%, 137.06%.

In summary, during the overtaking process of right-turning vehicles and straight-going vehicles, the change of turning radius has the greatest impact on the yaw torque of car B: the turning radius increases by 80%, and the maximum yaw torque of car B increases by 137.06%, which adversely affects the stability and safety of car B.

## 6. Conclusion

In this paper, the dynamic grid technology of elastic smoothing and grid reconstruction is used to simulate the overtaking process of right-turning vehicles and straight-going vehicles, and the aerodynamic variation law is obtained. There are three main points:

- (1) During the overtaking process, the two lateral force peaks of the right-turning vehicle are reduced to varying degrees compared with the right-turning process of the single vehicle, and the second lateral force peak appears earlier.
- (2) With the increase of the speed of the straight-going vehicle, the yaw moment of the two vehicles and the lateral force of the straight-moving vehicle increases linearly, but the lateral force of the right-turning vehicle decreases first and then increases.
- (3) With the increase of the turning radius, the lateral force of the two vehicles and the yaw moment of the straight car decreased linearly, but the yaw moment of the right-turning car increased linearly.

## References

- Ahmed F. Abdel Azim and Ahmed F. Abdel Gawad, (2000). A Flow Visualization Study of the Aerodynamic Interference Between Passenger Cars, Sae World Congress, 2000-01-0355.
- C. Noger, C. REGARDIN and E. Széchényi, (2005). Investigation of the transient aerodynamic phenomena associated with passing manoeuvres. *Journal of Fluids and Structures*, 21(3), 231-241.
- Corin. R. J, He. L and Dominy. R. G., (2008). A CFD investigation into the transient aerodynamic forces on overtaking road vehicle models. *Journal of Wind Engineering & Industrial Aerodynamics*, 96(8-9), 1390-1411.
- FU Limin, He Baoqin, Wu Yunzhu, Hu Xingjun, Zhang Yingchao, (2007). Study of aerodynamic characteristics of automobile overtaking process. *Acta Aerodynamica Sinica*, (03), 351-356.
- Howell. J, Garry. K and Holt. J., (2014). The Aerodynamics of a Small Car Overtaking a Truck. *SAE International Journal of Passenger Cars—Mechanical Systems*, 7(2), 626-638.

- Hu Xingjun, Yang Bo, Wang Jingyu, Zhang Yingchao, (2010). Dynamic Simulation of Influence of lateral Distance on Automotive Aerodynamic Characteristics during Overtaking, SAE-C2010C180, 1407-1411.
- Kieffer W, Moujaes S and Armbya N., (2006). CFD study of section characteristics of Formula Mazda race car wings. *Mathematical and Computer Modelling*, 43(11-12), 1275-1287.
- TANG Hongtao, Long Shijie, Yang juncheng, Wang Xu, (2020). Vehicle aerodynamic properties during lane-changing and overtaking based on CFD simulation. *Chinese Journal of Automotive Engineering*, 10(04), 269-280.
- TANG Hongtao, YANG Juncheng, ZHANG Xiang, LIU Xuelong, (2022). Aerodynamic Characteristics Analysis of Overtaking Process on Two-Lane Roads Based on CFD Simulation. *Chinese Journal of Automotive Engineering*, 12(03), 254-266.
- Wu Yunzhu, He Baoqin, FU Limin, (2007). Influence of velocity on transient aerodynamic characteristics of overtaking and overtaken vehicles. *Journal of Jilin University (Engineering and Technology Edition)*, (05), 1009-1013.

### Copyrights

Copyright for this article is retained by the author(s), with first publication rights granted to the journal.

This is an open-access article distributed under the terms and conditions of the Creative Commons Attribution license (<http://creativecommons.org/licenses/by/4.0/>).